Journal of Microscopy and Ultrastructure 4 (2016) 76–84

Contents lists available at ScienceDirect

Journal of Microscopy and Ultrastructure

journal homepage: www.elsevier.com/locate/jmau

Original Article

Nigella sativa oil alleviates ultrastructural alterations induced by tramadol in rat motor cerebral cortex

Nesreen Moustafa Omar*

Department of Histology and Cell Biology, Faculty of Medicine, Mansoura University, Mansoura, Egypt

ARTICLE INFO

Article history:
Received 23 August 2015
Received in revised form 1 November 2015
Accepted 2 December 2015
Available online 15 December 2015

Keywords:
cerebral cortex
Nigella sativa
tramadol
ultrastructure

ABSTRACT

Tramadol is an opioid analgesic used to alleviate acute and chronic pain. *Nigella sativa* oil is one of the traditional remedies with antioxidant activity. This study was designed in order to investigate the ultrastructural alterations induced by tramadol in the rat cerebral cortex and to find out any possible protective effect of *N. sativa* oil against these alterations. Twenty-four male albino rats were assigned to three groups. Group I received intraperitoneal and oral normal saline for 30 days. Group II received intraperitoneal injections of tramadol 20 mg/kg/day, 40 mg/kg/day and 80 mg/kg/day on the first, second and third 10 days of the study, respectively. Group III received intraperitoneal tramadol similar to Group II and oral *N. sativa* oil at a dose of 4 ml/kg/day for 30 days. Specimens from the motor area were obtained and processed for transmission electron microscopy. In the tramadol-treated group, pyramidal and granular cells appeared shrunken and showed ultrastructural features of apoptosis such as nuclear membrane invaginations, chromatin margination, dilated rough endoplasmic reticulum, dilated Golgi saccules, and mitochondria with disintegrated cristae. The myelinated axons showed disorganization and splitting of the myelin sheath and contained vacuoles and abnormal mitochondria. Administration of *N. sativa* oil partially protected the cortical neurons and myelinated axons against tramadol-induced changes. In conclusion, *N. sativa* oil alleviates ultrastructural apoptotic changes induced by tramadol in the rat motor cerebral cortex.

1. Introduction

The opioid analgesic tramadol has been used to alleviate acute and chronic pain [1]. It has been prescribed in many pathological conditions, for example, motor neuron disease, rheumatoid arthritis and management of labor pain [2].

The structure of tramadol is similar to codeine and has analgesic potency lower than that of morphine [3]. Tramadol acts on nonadrenergic and serotonergic systems. Therefore, it is effective in the treatment of depression, anxiety and phobias [4,5]. Various tramadol adverse reactions such as nausea, vomiting, sweating, itching, constipation and psychological and physical addiction have been reported [6,7].

In Arabian countries, *Nigella sativa* is commonly used as traditional medicine for treatment of many pathological conditions [8]. *N. sativa* has immunomodulatory, anti-inflammatory and antihistaminic effects [9,10]. Antioxidant and anti-eicosanoid activities of the fixed oil of *N. sativa* have been previously described [11]. Most of the biological activity of *N. sativa* has been found to be due to thymoquinone, which is a pharmacologically active

* Corresponding author. Department of Histology and Cell Biology, Faculty of Medicine, Mansoura University, 35516, Mansoura, Egypt. Tel.: +201006450090; fax: +20502397900.
E-mail address: nesrinemoustafa@gmail.com (N.M. Omar).

http://dx.doi.org/10.1016/j.jmau.2015.12.001
2213-879X/

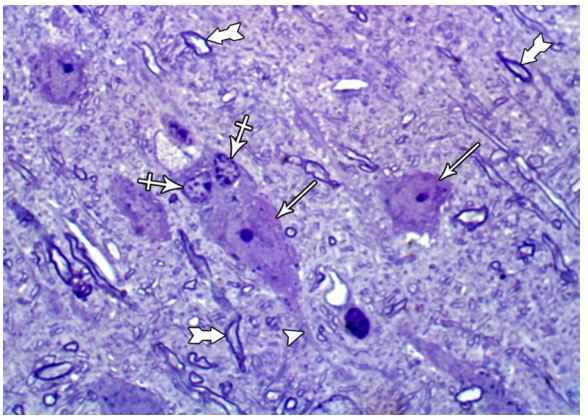

Figure 1. A semithin section of control rat cerebral cortex showing pyramidal cells (arrows), apical dendrite (arrowhead), perineural neuroglia (crossed arrows), and myelinated axons (tailed arrows). Stain: toluidine blue; magnification: 1000×.

quinone and has analgesic and anti-inflammatory activities [12].

The effect of tramadol on the cerebral cortex has been previously investigated; however, few studies have demonstrated its effect on the ultrastructure of the rat motor cortex. Therefore, this study was designed to demonstrate the ultrastructural alterations caused by tramadol in the rat cerebral cortex and to investigate whether or not treatment with *N. sativa* oil (NSO) could alleviate such changes.×

2. Materials and methods

2.1. Chemicals

Tramadol hydrochloride was obtained from (ADWIA, Ramadan City, Egypt) as 20-mg ampoules. *N. sativa* extract volatile oil was purchased from Pharco (Alexandria, Egypt) as 100-mg capsules.

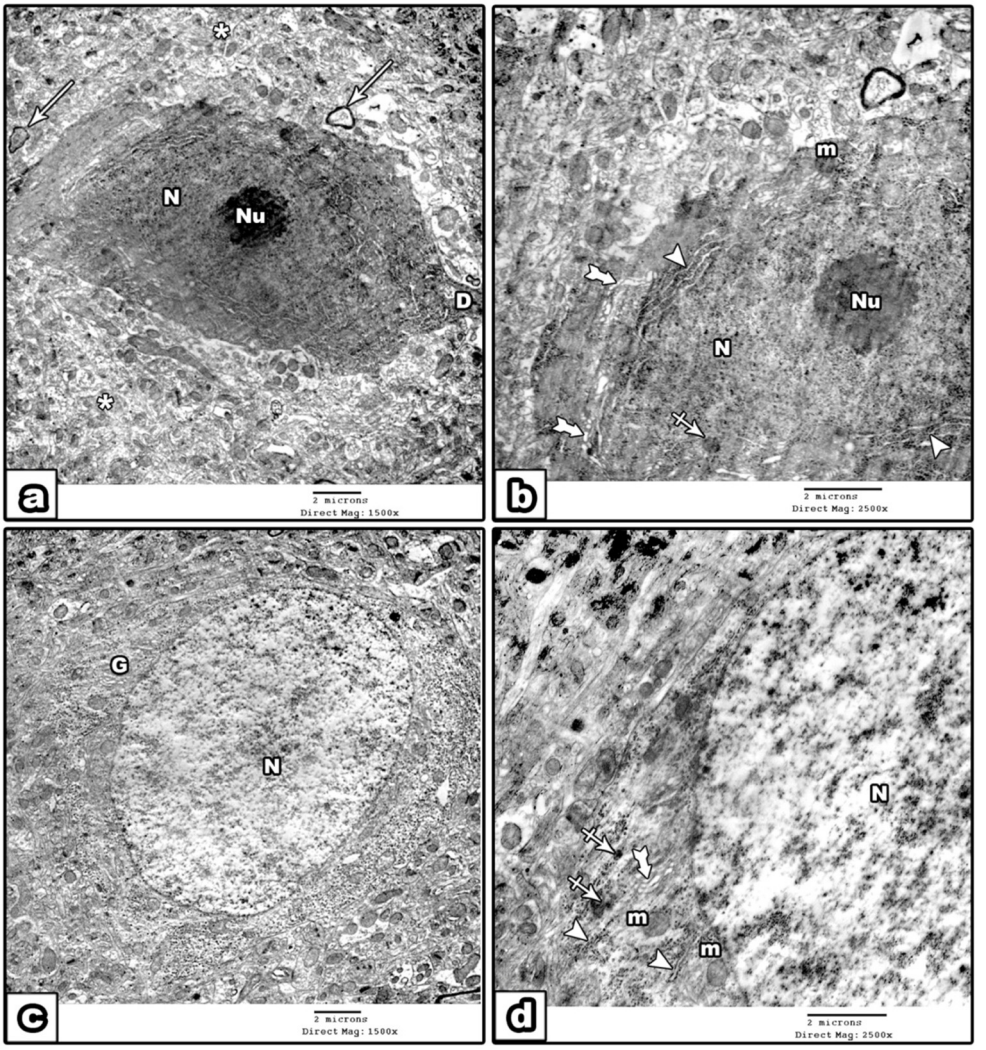

Figure 2. Electron micrographs of the cerebral cortex of control rat. (a,b) a pyramidal cell with a vesicular nucleus (N), prominent nucleolus (Nu), apical dendrite (D), mitochondria (m), rER (arrowheads), Golgi saccules (tailed arrows) and a lysosome (crossed arrow). Note also neuropil (*) and myelinated axons (arrows). (c, d) A granular cell (G) with highly vesicular nucleus (N), mitochondria (m), rER (arrowheads), lysosomes (crossed arrows) and Golgi saccules (tailed arrow). Magnification: a, c, 1500×; b, d, 2500×.

2.2. Animals

The experimental protocol of the study was designed according to the rules approved by the Ethical Committee of the Faculty of Medicine, Mansoura University, Egypt. Animals were maintained and used in accordance with the Animal Welfare Act and the Guide for the Care and Use of MERC (Mansoura Experimental Research Center). Twenty-four male albino rats of average weight 180–220 g were kept in an adequately ventilated room at 22 °C and 25 °C, under a regular 12-hour light/12-hour dark cycle and given food and water *ad libitum*.

2.3. Animal grouping

The animals were randomly assigned to three equal groups. Group I (control group) received normal intraperitoneal and oral saline for 30 days. Group II (tramadol-treated group) received repeated intraperitoneal injections of increasing doses of tramadol of 20 mg/kg/day, 40 mg/kg/day and 80 mg/kg/day on the first, second, and third 10 days of the study, respectively. The dose of tramadol was equivalent to that used in a previous study [13]. Group III (tramadol + NS-treated group) received intraperitoneal tramadol at doses similar to those of Group II. In addition, *N. sativa* extract volatile oil was administered orally at a dose of 4 ml/kg/day, 30 minutes before each tramadol injection for 30 days. The dose of the oil was detected in accordance with a previous work [14].

2.4. Histological study

All animals were anesthetized using intraperitoneal sodium pentobarbital (40 mg/kg). Animal perfusion was done through the left ventricle. Small fragments (1 mm^3) from the left motor area were rapidly obtained and immediately fixed in 0.1 mol/L phosphate buffer containing 2.5% glutaraldehyde and 2% paraformaldehyde at 4 °C overnight. Specimens were postfixed in 1% osmium tetroxide for 1 hour at 4 °C and washed three times in phosphate-buffered saline (10 minutes each). Specimens were dehydrated in graded ethanol and cleared in acetone. The specimens were immersed in equal volumes of Epon and acetone for 1 hour, followed by acetone: Epon (25:50) for 1 hour. Finally, the specimens were immersed in Epon only in embedding capsules and placed in the oven at 60 °C overnight for polymerization. Semithin sections (1 μm) were cut by ultramicrotome (Ultracut UCT; Leica, Germany) and stained with 1% toluidine blue. Ultrathin sections (60–80 nm) were cut and stained with 2% uranyl acetate for 10 minutes, followed by Reynold's lead citrate for 10 minutes. Ultrathin sections were examined and photographed using a JEOL-JEM-100 SX transmission electron microscope [15] in the Electron Microscopy Unit, Tanta University, Egypt.

2.5. Statistical analysis

Using the semithin sections, shrunken pyramidal cells were counted in 10 high-power fields (1000 ×) for each group. To assess the degree of axon circularity, 10 axons from electron micrographs of each group were manually extracted and index of circularity (IC) for the myelinated axons was measured using Image J software. IC was calculated as the ratio between the surface area of the myelinated axon and the area of a circle having the same perimeter [16]. The collected data were analyzed using SPSS version 16. Student's *t* test was used to compare the studied groups. The results were presented as mean ± standard deviation and $p \leq 0.05$ was considered significant.

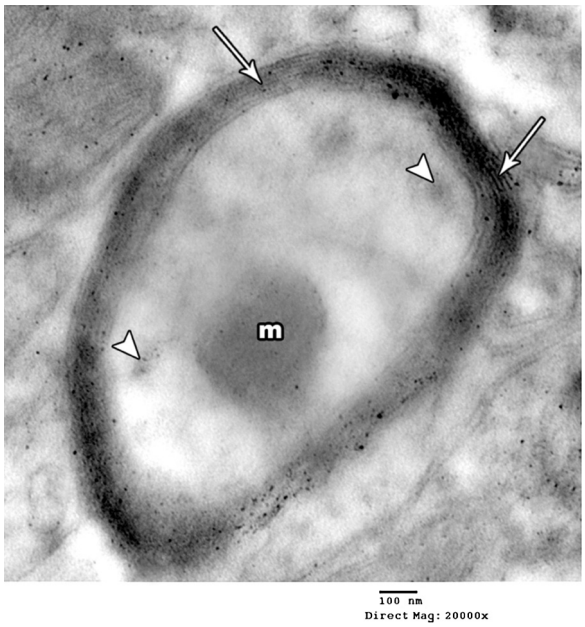

Figure 3. An electron micrograph of control rat cerebral cortex showing a myelinated axon with a smooth regular contour and regular arrangement of myelin lamellae (arrows). The axoplasm contains a mitochondrion (m) and neurofibrils (arrowheads). Magnification: 20,000×.

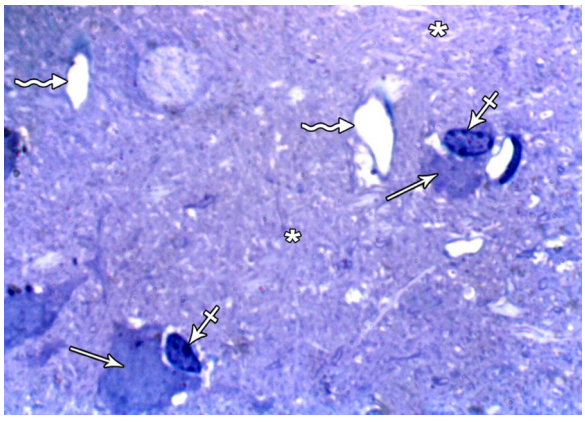

Figure 4. A semithin section of tramadol-treated rat cerebral cortex showing shrunken pyramidal cells (arrows), perineural neuroglia (crossed arrow) and dilated capillaries (wavy arrows). Note ill-defined myelinated axons in the neuropil (*). Stain: toluidine blue; magnification: 1000×.

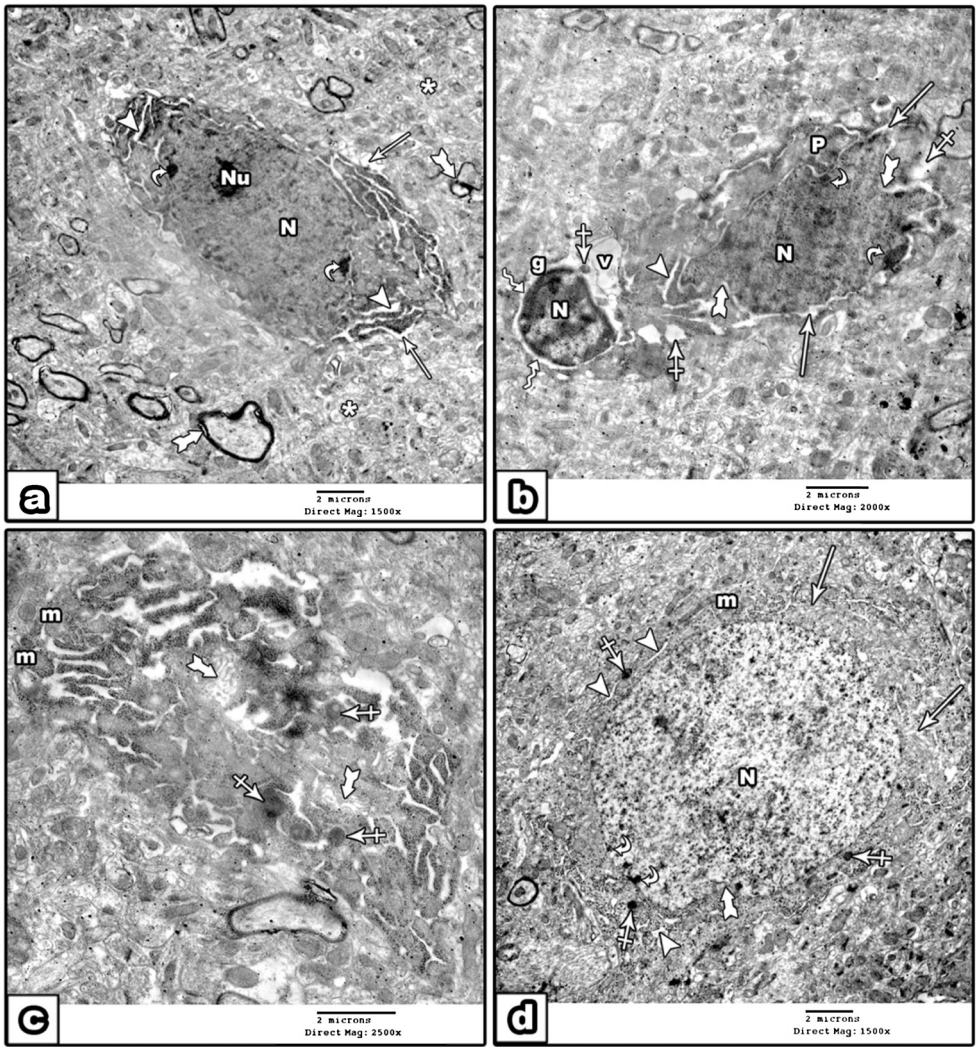

Figure 5. Electron micrographs of Tramadol-treated rat cerebral cortex. (a) Shrunken pyramidal cell with a wide perineural space (arrows), nucleus (N), nucleolus (Nu), chromatin margination (curved arrows) and dilated rER (arrowheads). Note irregular outline of myelinated axons (tailed arrows) in the neuropil (*). (b) Apoptotic pyramidal cell (p) with wide perineural space (crossed arrows), nucleus (N), wide perinuclear space (arrows), nuclear membrane invaginations (tailed arrows), chromatin margination (curved arrows) and dilated rER (arrowhead). A perineural neuroglia (g) shows a hyperchromatic nucleus (N), wide perinuclear space (wavy arrows), a lysosome (crossed arrow) and a large cytoplasmic vacuole (v). (c) Degenerated pyramidal cell with complete loss of cytoarchitecture. The cytoplasm appears dense and shows many lysosomes (crossed arrows), mitochondria with disintegrated cristae (m) and dilated and vesiculated Golgi saccules (tailed arrows). (d) A shrunken granular cell showing a nucleus (N), nuclear membrane invagination (tailed arrow), clumps of marginated chromatin (curved arrows), mitochondria (m), lysosomes (crossed arrows), dilated rER (arrowheads) and dilated Golgi saccules (arrows). Magnification: a, d, 1500×; b, 2000×; c, 2500×.

3. Results

3.1. Histological results

3.1.1. Control group

Examination of semithin sections of control rat motor cortex demonstrated the inner pyramidal layer containing large pyramidal cells scattered in a background of neuroglia formed of neuroglia cells and myelinated axons (Figure 1). By electron microscopy, the pyramidal cells were characterized by vesicular nuclei with prominent nucleoli and apical dendrites (Figure 2a). The cytoplasm showed rough endoplasmic reticulum (rER), mitochondria, lysosomes and Golgi apparatus (Figure 2b). Granular cells were also demonstrated. They appeared rounded with highly vesicular rounded nuclei (Figure 2c). The cytoplasm contained rER, ribosomes, mitochondria, Golgi apparatus and lysosomes (Figure 2d). The myelinated axons showed smooth regular contours and regular arrangement of the myelin lamellae and the axoplasm contained mitochondria and neurofibrils (Figure 3).

3.1.2. Tramadol-treated group

Examination of semithin sections of tramadol-treated rat motor cortex revealed shrunken pyramidal cells, perineural neuroglia, dilated blood capillaries and ill-defined myelinated axons (Figure 4). In the ultrathin sections, pyramidal cells appeared shrunken with wide perineural

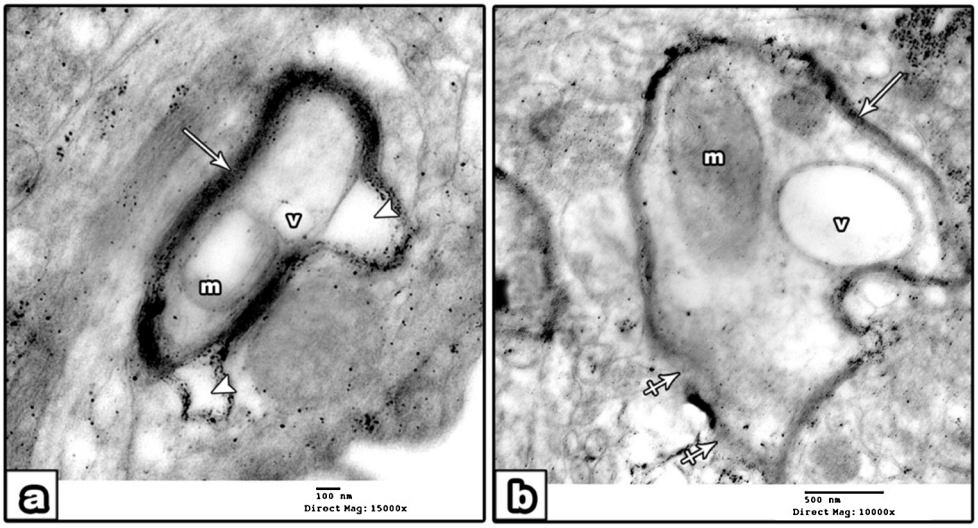

Figure 6. Electron micrographs of tramadol-treated rat cerebral cortex showing two myelinated axons (arrows). (a) Splitting (arrowheads) of myelin lamellae, swollen mitochondria (m) with disrupted cristae and a cytoplasmic vacuole (v). (b) Irregular outline with focal interruption (crossed arrows) of myelin sheath, mitochondria (m) and a large vacuole (v). Magnification: a, 15,000×; b, 10,000×.

spaces. The nuclei showed nuclear membrane invaginations and margination of chromatin and the cytoplasm contained dilated rER (Figures 5a and 5b). The perineural neuroglia also showed nuclear condensation with wide perinuclear spaces, lysosomes and cytoplasmic vacuoles (Figure 5b). Some of the pyramidal cells appeared degenerated with complete loss of cytoarchitecture. The cytoplasm appeared dense and contained many lysosomes, vesiculated and dilated Golgi saccules, and damaged mitochondria (Figure 5c). The granular cells were also shrunken and showed invagination of the nuclear membrane and clumps of marginated chromatin. The cytoplasm contained many lysosomes, dilated rER and dilated Golgi saccules (Figure 5d). The myelinated axons were irregular in outline and showed splitting or discontinuity of myelin sheaths. The axoplasm contained vacuoles and mitochondria with disrupted cristae (Figures 5a and 6).

3.1.3. *Tramadol + NS-treated group*

In the semithin sections, the motor cortex of this group showed apparently normal pyramidal cells, however, few degenerated pyramidal cells were seen (Figure 7). The ultrastructural study revealed that most of the pyramidal cells were similar to the control group with vesicular nuclei and prominent nucleoli. The cytoplasm contained well-developed rER, numerous ribosomes, lysosomes, well-developed Golgi, and intact elongated mitochondria (Figures 8a and 8b). However, occasional degenerated pyramidal cells with dark folded nuclei, dilated rER, lysosomes and dilated Golgi saccules were still demonstrated (Figure 8c). The granular cells appeared normal and had similar structure to the control group. The nuclei were highly vesicular with regular contours and the cytoplasm showed a well-developed rER, numerous ribosomes, intact rounded and elongated mitochondria, lysosomes and Golgi apparatus (Figure 9). Myelinated axons appeared similar to those in the control group with smooth regular contours and regular arrangement of myelin lamellae. However, focal splitting of myelin sheaths and damaged mitochondria were still observed (Figure 10).

3.2. *Statistical analysis*

The mean number of shrunken pyramidal cells/high-power field was significantly increased in Group II compared to the Control Group ($p < 0.001$). This number was significantly decreased in Group III compared to Group II ($p < 0.01$), however, it was still higher than in the Control Group (Figure 11). IC was significantly decreased ($p < 0.01$) in Group II compared to Groups I and III (Figure 12).

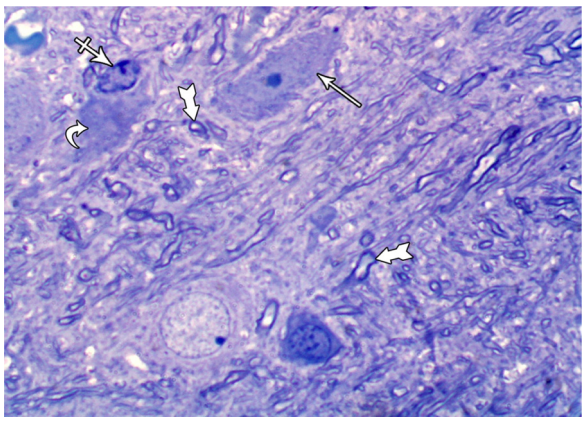

Figure 7. A semithin section of tramadol + NS-treated rat cerebral cortex showing an apparently normal pyramidal cell (arrow), a shrunken pyramidal cell (curved arrow), a perineural neuroglia (crossed arrow) and myelinated axons (tailed arrows). Stain: toluidine blue; magnification: 1000×.

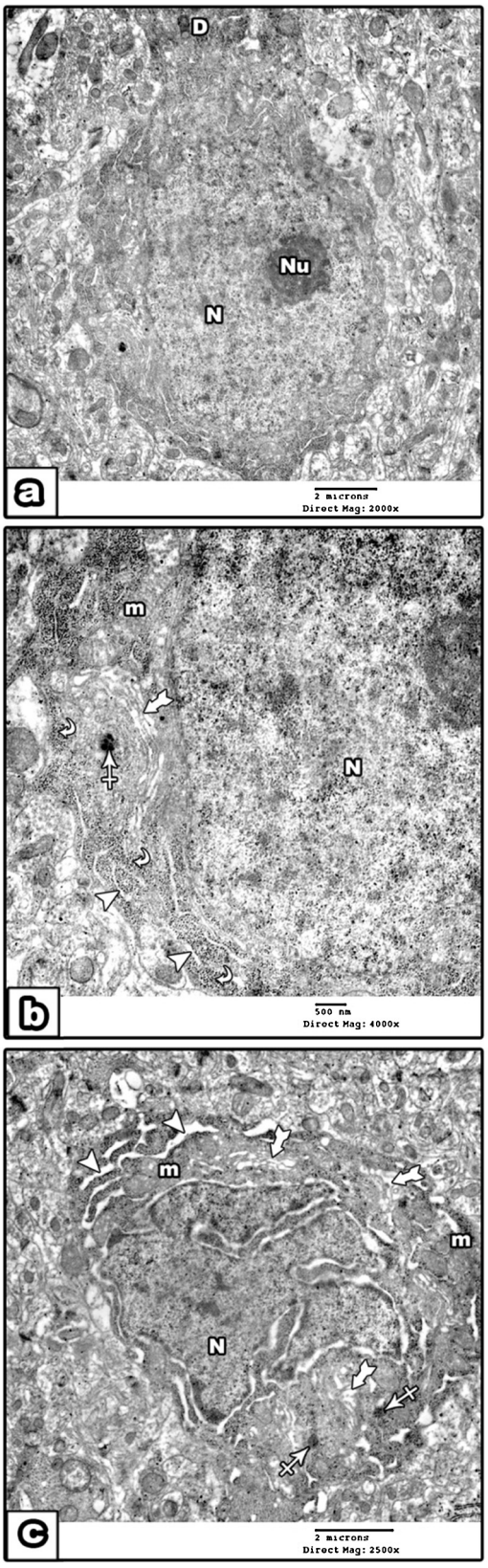

4. Discussion

The tramadol-treated group had degenerated shrunken neurons and neurons with ultrastructural features of apoptotic cell death in the form of nuclear invagination, chromatin margination, dilated rER cisternae, and abnormal mitochondria. It has been reported that early-phase apoptosis is characterized by invagination of the nuclear membrane. In the late phase, the chromatin becomes condensed and segregated along the margin of the nuclear membrane, and the cytoplasm shows densely packed organelles, including mitochondria and electron-dense vesicles [17]. Similar ultrastructural changes indicating apoptosis were observed in the brain of monkeys and rats with drug-induced and septic neurotoxicity [18,19]. Red neuron degeneration and apoptosis were also found in the brains of rats with chronic use of morphine and opioids [13,20].

Abnormal mitochondria were also observed in the neurons and axons of the tramadol-treated group. The mitochondrial changes observed in this study may be an early sign of apoptosis and a mechanism by which the cell adapts to an unfavorable environment, such as free radicals [21]. High doses of tramadol inhibit Complexes I, III and IV of the electron transfer chain in mitochondria. The inhibition of Complex III leads to generation of reactive oxygen species [22]. The decrease in the mitochondrial membrane potential following mitochondrial damage leads to release of apoptosis-inducing factors, resulting in activation of caspase proteases that cause nuclear condensation and cytoplasmic fragmentation [23].

Tramadol administration induces oxidative stress and a significant decrease in the antioxidants in brain tissue [14,24]. Also, tramadol induces inflammatory reactions that may be the cause of oxidative stress by changing cell membrane fatty acid composition [25]. The brain is highly susceptible to oxidative damage because it has high oxygen consumption, high concentration of polyunsaturated fatty acids and low levels of antioxidants [26]. Oxidative stress causes protein modifications and carbonylation that result in loss of function and decrease of enzyme activity [27].

NO appears to be involved in the analgesic effect of tramadol [28]. The reaction between NO and superoxide results in peroxynitrite, which exerts its toxic effect via direct oxidative mechanisms [29]. Nitration of structural proteins such as neurofilaments and actin can disrupt filament assembly and induce pathological consequences [30]. Similarly, long-term use of opioids can affect the neuronal cytoskeleton and induce neuronal damage [31]. Moreover, splitting and irregular contours of myelin reported in tramadol-treated rats can be explained by myelin damage

Figure 8. Electron micrographs of the cerebral cortex of tramadol + NS-treated rat. (a, b) Pyramidal cell with vesicular nucleus (N), prominent nucleolus (Nu) and apical dendrite (D), intact elongated mitochondria (m), rER (arrowheads), numerous ribosomes (curved arrows), a well-developed Golgi apparatus (tailed arrow) and lysosomes (crossed arrow). (c) Shrunken pyramidal cell showing dark highly folded nucleus (N), dilated rER (arrowheads), dilated Golgi saccules (tailed arrows), lysosomes (crossed arrows) and mitochondria (m) with mild cristolysis. Magnification: a, 2000×; b, 4000×; c, 2500×.

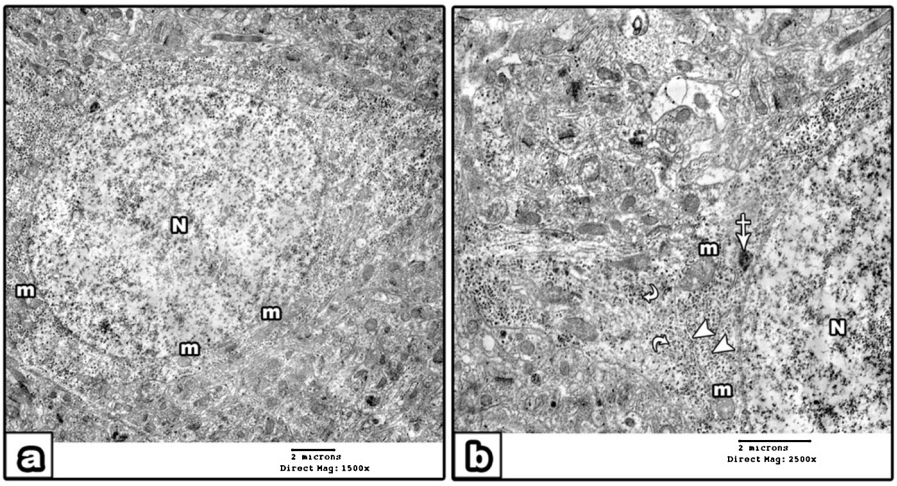

Figure 9. Electron micrographs of a granular cell in the cerebral cortex of tramadol + NS-treated rat showing highly vesicular nucleus (N), many rounded or elongated intact mitochondria (m), well developed rER (arrowheads), numerous ribosomes (curved arrows) and a lysosome (crossed arrow). Magnification: a, 1500×; b, 2500×.

caused by NO, decreased myelin-associated glycoprotein, or autoantibodies to myelin basic protein [32]. In addition, tramadol may affect the vascular endothelial cells, resulting in NO release, which has an endothelium-relaxing effect leading to vascular congestion, as observed in the cerebral cortex of tramadol-treated rats [33].

Marked reduction of ultrastructural apoptotic changes was observed in the cerebral cortex of Tramadol + NS-treated rats. Most neurons and axons appeared normal with intact mitochondria and rER. These findings indicate a protective effect of *N. sativa* oil against tramadol-induced cellular damage. This improvement may be due to the protective role of thymoquinone against oxidative damage induced by free radical generating pathology, as previously described [34,35]. It is reported that *N. sativa* oil possesses anti-inflammatory and immunomodulatory and

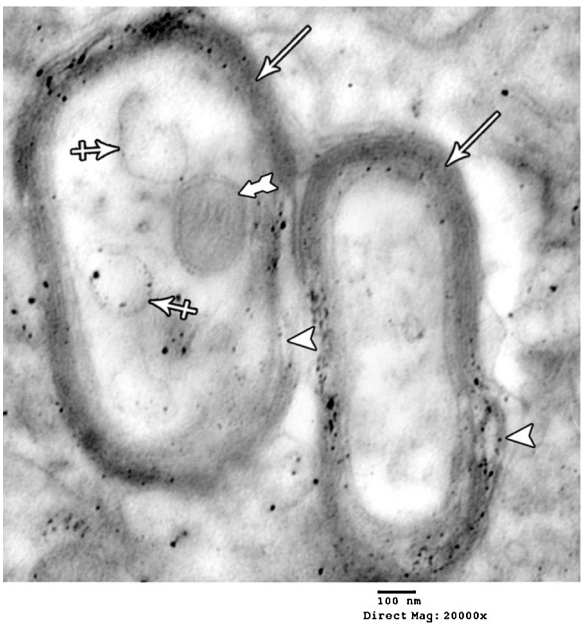

Figure 10. An electron micrograph of tramadol + NS-treated rat cerebral cortex showing two myelinated axons (arrows). Myelin sheaths appear intact except for areas of focal splitting (arrowheads) of myelin lamellae, the mitochondria are either intact (tailed arrow) or disrupted (crossed arrow). Magnification: 20,000×.

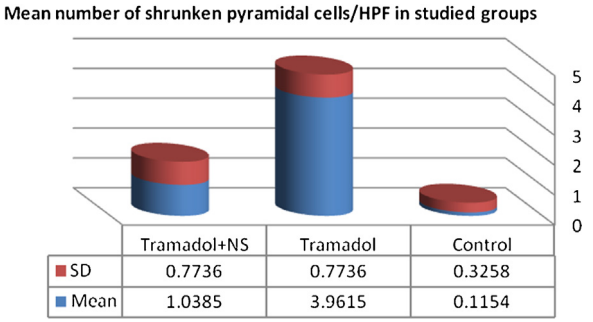

Figure 11. Mean number of shrunken pyramidal cells/high-power field in studied groups.

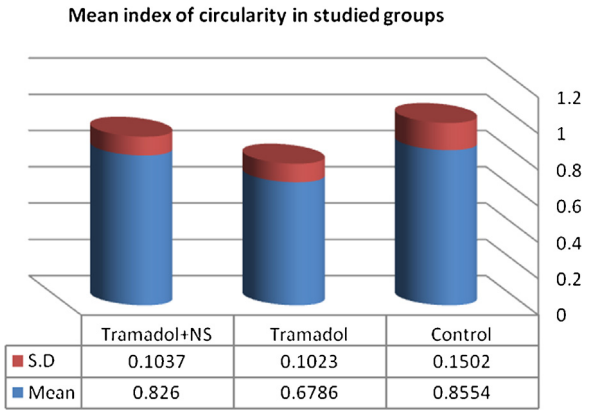

Figure 12. Mean index of circularity in studied groups.

antioxidant properties and thus decreases the oxidative stress caused by drugs and heavy metals [36,37]. Moreover, a protective role of thymoquinine against oxidative stress was also demonstrated in hippocampal neurodegeneration after chronic toluene exposure and in rat models of cerebral ischemia–reperfusion injury and subarachnoid hemorrhage [34,38,39]. The antioxidant activity of thymoquinone is due to inhibition of eicosanoid generation, namely thromboxane B2 and leukotriene B4 and could prevent membrane lipid peroxidation in the tissues [38,40]. In addition, *N. sativa* could inhibit NO production and expression of inducible NO synthase [41,42], which may be crucial mechanisms by which *N. sativa* oil protects against hazardous effects of tramadol on the cerebral cortex. In conclusion, tramadol administration results in many apoptotic ultrastructural changes in the cerebral cortex, which are markedly ameliorated by *N. sativa* oil.

Conflict of interest

The authors report no conflict of interest.

References

[1] Lee RC, McTavish, Sorkin EM. Tramadol: a preliminary review of its pharmacodynamic and pharmacokinetic properties and therapeutic potential in acute and chronic pain states. Drugs 1993;46:313–40.
[2] Matthiesen T, Wohrmann T, Coogan TP, Uragg H. The experimental toxicology of tramadol: an overview. Toxicol Lett 1998;95:63–71.
[3] Lehmann KA, Kratzenberg U, Schroeder-Bark B, Horrichs-Haermeyer G. Post-operative patient-controlled analgesia with tramadol: analgesia efficacy and minimum effective concentrations. Clin J Pain 1990;6:212–20.
[4] Gana TJ, Pascual ML, Fleming RR, Schein JR, Janagap CC, Xiang J, Vorsanger GJ. 023 Study Group. Extended-release tramadol in the treatment of osteoarthritis: a multicenter, randomized, double-blind, placebo-controlled clinical trial. Curr Med Res Opin 2006;22:1391–401.
[5] McKeon GP, Pacharinsak C, Long CT, Howard AM, Jampachaisri K, Yeomans DC, Felt SA. Analgesic effects of tramadol, tramadol–gabapentin, and buprenorphine in an incisional model of pain in rats (*Rattus norvegicus*). J Am Assoc Lab Anim Sci 2011;50:192–7.
[6] Kabel JS, Van Puijenbroek EP. Side effects of tramadol: 12 years of experience the Netherlands. Ned Tijdsch Geneeskd 2005;149:754–7.
[7] Lanier RK, Lofwall MR, Mintzer MZ, Bigelow GE, Strain EC. Physical dependence potential of daily tramadol dosing in humans. Psychopharmacol (Berl) 2010;211:457–66.
[8] Sayed MD. Traditional medicine in health care. J Ethnopharmacol 1980;2:19–22.
[9] Kanter M, Meral I, Yener Z, Ozbek H, Demir H. Partial regeneration/proliferation of the beta-cells in the islets of Langerhans by *Nigella sativa* L. in streptozotocin-induced diabetic rats. Tohoku J Exp Med 2003;201:213–9.
[10] Kanter M, Coskun O, Uysal H. The antioxidative and antihistaminic effect of *Nigella sativa* and its major constituent, thymoquinone on ethanol-induced gastric mucosal damage. Arch Toxicol 2006;80:217–24.
[11] Houghton PJ, Zaraka R, Delas Heras B, Hoult JR. Fixed oil of *Nigella sativa* and derived thymoquinone inhibit eicosanoid generation in leucocytes and lipid peroxidation. Planta Med 1995;47:119–26.
[12] Abdel-Fattah AM, Matsumoto K, Watanabe H. Antinociceptive effects of *Nigella sativa* oil and its major component, thymoquinone, in mice. Eur J Pharmacol 2000;400:89–97.
[13] Atici S, Cinel L, Cinel I, Doruk N, Aktekin M, Akca A, et al. Opioid neurotoxicity: comparison of morphine and tramadol in an experimental rat model. Int J Neurosci 2004;114:1001–11.
[14] Abdel-Zaher AO, Abdel-Rahman MS, Elwasei FM. Protective effect of *Nigella sativa* oil against tramadol-induced tolerance and dependence in mice: role of nitric oxide and oxidative stress. Neurotoxicology 2011;32:725–33.
[15] Woods AE, Stirling JW. Electron microscopy. In: Bancroft JD, Gamble M, editors. Theory and practice of histological techniques. 6th ed London, New York: Churchill Livingstone; 2008. p. 601–36.
[16] Vaitkeviciene I, Vaitkevicius R, Paipaliene P, Zekonis G. Morphometric analysis of pulpal myelinated nerve fibers in human teeth with chronic periodontitis and root sensitivity. Medicina (Kaunas) 2006;42:914–22.
[17] Tiso M, Gangemi R, Bargellesi Severi A, Pizzolitto S, Fabbi M, Risso A. Spontaneous apoptosis in human thymocytes. Am J Pathol 1995;147:434–44.
[18] Zou X, Patterson TA, Sadovova N, Twaddle NC, Doerge DR, Zhang X, et al. Potential neurotoxicity of ketamine in the developing rat brain. Toxicol Sci 2009;108:149–58.
[19] Kafa IM, Uysal M, Bakirci S, Kurt A. Sepsis induces apoptotic cell death in different regions of the brain in a rat model of sepsis. Acta Neurobiol Exp (Warsz) 2010;70:246–60.
[20] Sharifipour M, Izadpanah E, Nikkhoo B, Zare S, Abdolmaleki A, Hassanzadeh K, et al. A new pharmacological role for donepezil: attenuation of morphine-induced tolerance and apoptosis in rat central nervous system. J Biomed Sci 2014;23:21–6.
[21] Wakabayashi T. Megamitochondria formation-physiology and pathology. J Cell Mol Med 2002;6:497–538.
[22] Lemarie A, Grimm S. Mutations in the heme b-binding residue of SDHC inhibit assembly of respiratory chain complex II in mammalian cells. Mitochondrion 2009;9:254–60.
[23] Zamzami N, Marchetti P, Castedo M, Decaudin D, Macho A, Hirsch T, et al. Sequential reduction of mitochondrial transmembrane potential and generation of reactive oxygen species in early programmed cell death. J Exp Med 1995;182:367–77.
[24] El-Gaafarawi II. Biochemical toxicity induced by tramadol administration in male rats. Egypt J Hosp Med 2006;23:353–62.
[25] Alici HA, Ozmen I, Cezur M, Sahin F. Effect of the spinal drug tramadol on the fatty acid compositions of rabbit spinal cord and brain. Biol Pharm Bull 2003;26:1403–6.
[26] Butterfield DA, Castegna A, Lauderback CM, Drake J. Evidence that amyloid beta-peptide-induced lipid peroxidation and its sequelae in Alzheimer's disease brain contribute to neuronal death. Neurobiol Aging 2002;23:655–64.
[27] Butterfield DA, Reed T, Newman SF, Sultana R. Roles of amyloid beta-peptide-associated oxidative stress and brain protein modifications in the pathogenesis of Alzheimer's disease and mild cognitive impairment. Free Radic Biol Med 2007;43:658–77.
[28] Dal D, Salman A, Salman E, Alper B, Aypar U. The involvement of nitric oxide on the analgesic effect of tramadol. Eur J Anaesthesiol 2006;23:173–80.
[29] Beckman JS, Beckman TW, Chen J, Marshall PA, Freeman BA. Apparent hydroxyl radical production by peroxynitrite: implication for endothelial injury from nitric oxide and superoxide. Proc Natl Acad Sci USA 1990;87:1620–4.
[30] Beckman JS, Koppenol WH. Nitric oxide, superoxide, and peroxynitrite the good, the bad, and the ugly. Am. J. Physiol 1996;271:C1424–37.
[31] Liu LW, Lu J, Wang XH, Fu SK, Li Q, Lin FQ. Neuronal apoptosis in morphine addiction and its molecular mechanism. Int J Clin Exp Med 2013;6:540–5.
[32] Hernández Fonseca JP, Rincón J, Pedreañez A, Viera N, Arcaya JL, Carrizo E. Structural and ultrastructural analysis of cerebral cortex, cerebellum and hypothalamus from diabetic rats. Exp Diabet Res 2009, http://dx.doi.org/10.1155/2009/329632.
[33] Jana M, Liu X, Koka S, Ghosh S, Petro TM, Pahan K. Ligation of CD40 stimulates the induction of nitric-oxide synthase in microglial cells. J Biol Chem 2001;276:44527–33.
[34] Kanter M. *Nigella sativa* and derived thymoquinone prevent hippocampal neurodegeneration after chronic toluene exposure in rats. Neurochem Res 2008;33:579–88.
[35] Radad K, Moldzio R, Taha M, Rausch WD. Thymoquinone protects dopaminergic neurons against MPP+ and rotenone. Phytother Res 2009;23:696–700.
[36] Mansour MA, Ginawi OT, El-Hadiyah T, El-Khatib AS, Al-Shabanah OA, Al-Sawaf HA. Effects of volatile oil constituents of *Nigella sativa* on carbon tetrachloride induced hepatotoxicity in mice: evidence for antioxidant effects of thymoquinone. Res Commun Mol Pathol Pharmacol 2001;110:239–51.
[37] Mousa AM, Salem MM, El-Mahalaway AM. Effect of thymoquinone on cadmium-induced toxicity of Leydig cells in adult male albino rats: a histological, immunohistochemical, and biochemical study. Egypt J Histol 2015;38:308–16.
[38] Hosseinzadeh H, Parvardeh S, Asl MN, Sadeghnia HR, Ziaee T. Effect of thymoquinone and Nigella sativa seeds oil on lipid peroxidation

level during global cerebral ischemia-reperfusion injury in rat hippocampus. Phytomedicine 2007;14:621–7.
[39] Ersahin M, Toklu HZ, Akakin D, Yuksel M, Yegen BC, Sener G. The effects of Nigella sativa against oxidative injury in a rat model of subarachnoid hemorrhage. Acta Neurochir (Wien) 2011;153:333–41.
[40] Mansour MA, Nagi MN, El-Khatib AS, Al-Bekairi AM. Effects of thymoquinone on antioxidant enzyme activities, lipid peroxidation and DT-diaphorase in different tissues of mice: a possible mechanism of action. Cell Biochem Funct 2002;20:143–51.
[41] Mahmood MS, Gilani AH, Khwaja A, Rashid A, Ashfaq MK. The *in vitro* effect of aqueous extract of *Nigella sativa* seeds on nitric oxide production. Phytother Res 2003;17:1–5.
[42] El-Mahmoudy A, Matsuyama H, Borgan MA, Shimizu Y, El-Sayed MG, Minamoto N, et al. Thymoquinone suppresses expression of inducible nitric oxide synthase in rat macrophages. Int Immunopharmacol 2002;2:1603–11.